

Fast Response MR-Fluid Actuator*

Naoyuki TAKESUE**, Junji FURUSHO*** and Yuuki KIYOTA****

Magnetorheological (MR) fluids are materials that change their rheological behavior upon applying a magnetic field. They have been promising as functional fluids that can improve the properties of mechanical systems. We have developed an actuator using MR fluid. In the previous paper, a method of designing MR-fluid actuators was proposed on the basis of magnetic circuit theory. The basic experiments were carried out and static properties that agreed well with the design were obtained. However, the transient response, which was not considered in the design phase, was not very fast. In this study, we investigate the dynamics of the MR-fluid actuator and aim to improve the response. The transient magnetic analysis is examined in consideration of the eddy current. Two approaches to improving the response are proposed. Finally, we realize a much faster MR-fluid actuator.

Key Words: Actuator, Finite Element Method, Human Interface, Identification, MR Fluid, Magnetic Field, Eddy Current, Response

1. Introduction

Magnetorheological (MR) fluid⁽¹⁾⁻⁽⁴⁾, which is known as a functional fluid, changes its rheological characteristics upon the application of a magnetic field. Since the MR fluid causes the maximum yield stress of about 50 to 100 kPa, and it responds within several milliseconds, it has attracted much attention as a new material for improving mechanical systems and has been studied by numerous researchers⁽⁵⁾⁻⁽¹⁴⁾.

We have developed a clutch which can control the transmitted torque according to a magnetic field, by using MR fluid⁽¹⁵⁾⁻⁽¹⁸⁾. An MR-fluid actuator that consists of an input component, the clutch and an output component, was proposed. The MR-fluid actuator realizes both low inertia and high torque. Since the input speed is mechanically limited and the inertia on the output side is small,

any system using it is safe for human interaction. Therefore, equipment with which humans interact directly, such as force display systems, are suitable targets of application for MR-fluid actuators.

In the previous paper⁽¹⁸⁾, we proposed a method of designing MR-fluid actuators on the basis of magnetic circuit theory and examined basic experiments of an actuator developed based on this design method. The results showed that the static properties agreed well with the designed properties. However, the transient property, which was not considered in the design phase, was not very fast. Then we improved the dynamic response by a torque feedback control.

It is said that the response time of MR fluid itself is a few ms (around 1 to 2 ms)^{(4),(8),(10)}. On the other hand, some researchers have reported that the responses of equipment using MR fluids are not very fast^{(8),(9)}. In this study, we investigate the factors influencing the response of the MR-fluid actuator and improve its response.

The contents of this paper are as follows. In section 2, the measurements of coil current, magnetic flux density and output torque of the MR-fluid actuator are described, and the dynamic properties are clarified. In section 3, magnetic field analyses by FEM are presented. Magnetic flux lines are confirmed in the static analysis. Next, the transient analysis in consideration of the eddy current is examined, and the magnetic response and the distribution of eddy-current density are shown. In sections 4 and 5, two approaches are proposed for improving the responses: one reduces the eddy current by changing the material;

* Received 15th March, 2004 (No. 02-0727). Japanese Original: Trans. Jpn. Soc. Mech. Eng., Vol.69, No.681, C (2003), pp.1342-1349 (Received 6th June, 2002).

** Graduate School of Engineering, Osaka University, 2-1 Yamadaoka, Suita-shi, Osaka 565-0871, Japan. (Currently: Nagoya Institute of Technology, Gokiso-cho, Showa-ku, Nagoya-shi, Aichi 466-8555, Japan. E-mail: takesue@nitech.ac.jp)

*** Graduate School of Engineering, Osaka University, 2-1 Yamadaoka, Suita-shi, Osaka 565-0871, Japan. E-mail: furusho@mech.eng.osaka-u.ac.jp

**** Yaskawa Electric Corporation, 2-1 Kurosaki-shiroishi, Yahatanishi-ku, Kitakyushu-shi, Fukuoka 806-0004, Japan

the other reduces the counter-magnetic flux. It is shown that these approaches improve the response time significantly by simulation analyses and experiments. Finally in section 6, basic experiments are carried out on the improved MR-fluid actuator, and the work is summarized in section 7.

2. Dynamics of MR-Fluid Actuator

2.1 Mechanism of MR-fluid actuator

The cross section of the MR-fluid actuator developed in the previous study is illustrated in Fig. 1. In the figure, the motor that drives the input component is omitted except for the shaft. The housing, the input component, the output component and MR fluid are distinguished with different shadings.

The input component is rotated by the motor via the gear. When magnetic field is applied between the input and output components, the torque is transmitted from the input component to the output component. Since the yield stress of the MR fluid changes according to the strength of the applied magnetic field, the output torque can be controlled by adjusting the coil current. For details, refer to our previous paper⁽¹⁸⁾.

2.2 Mechanism of torque generation

In the MR-fluid actuator, it can be considered that the torque is generated as follows:

- (1) A current is supplied to the coil according to the reference voltage input to the current amplifier.
- (2) A magnetomotive force is applied to the magnetic circuit by the coil current, and a magnetic field is generated.
- (3) The yield stress of the MR fluid is changed depending on the magnetic field strength, and the torque is output to the output shaft.

This is illustrated in Fig. 2. Note that the magnetic cir-

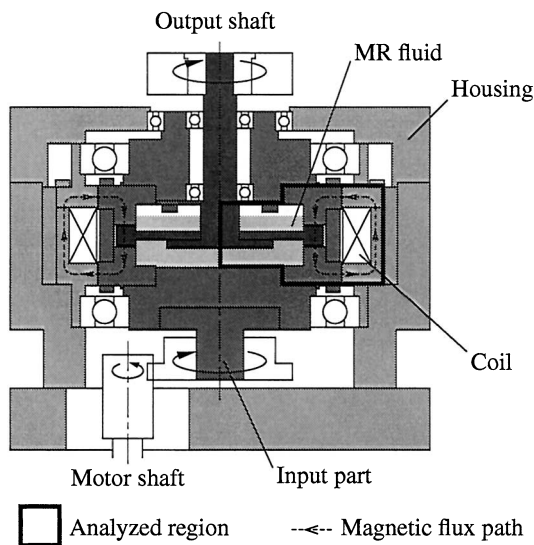


Fig. 1 Cross section of developed actuator

cuit is associated with all parts around the yoke involving the MR fluid, though the magnetic circuit and MR fluid are drawn separately in the diagram.

2.3 Comparison of measured response

The responses of coil current and output torque were measured in the previous work. It was shown that the time constant of the output torque response was very slow, about 45 ms, though the coil current responded within 1 ms.

In order to investigate the reason for the slow response, the response of the magnetic field, which may be strongly associated with torque generation, is measured experimentally. A Hall sensor is sandwiched between the input and output disks, and the magnetic response is measured. Then, the input and output components are stopped. Although this sensor measures the magnetic flux through the sensor itself, it cannot measure the flux through the MR fluid. However, the form of response of the magnetic circuit can be elucidated.

The measured magnetic flux density is shown in Fig. 3 together with the coil current and output torque. As

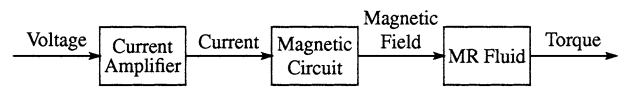


Fig. 2 Block diagram of MR-fluid actuator

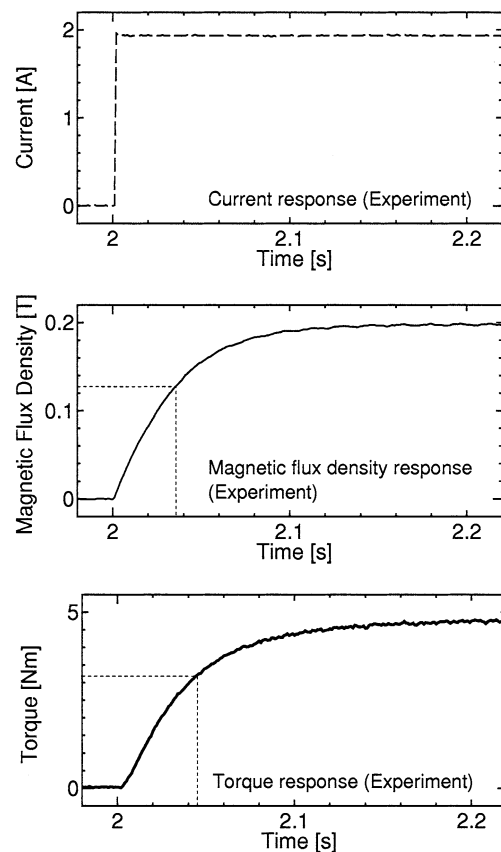


Fig. 3 Step responses of nominal MR-fluid actuator

seen from the figures, the time constant of the magnetic flux density is about 36 ms, which is not as fast as the current response. It can be said that the magnetic response should be improved first to improve the torque response.

3. Magnetic Analysis

3.1 Static analysis

First, a static analysis is performed by the finite element method (FEM). The analyzed region is shown with a thick line in Fig. 1. Materials used for the parts in the MR-fluid actuator are shown in Fig. 4. SS400, the rolled steel used for general structures, is used for the yoke which becomes the main path of magnetic flux. For the parts which should not be part of the magnetic path, aluminum alloy is used.

In simulation analysis, the width of an element of FEM was made less than 2 mm. The number of nodes was 940, and the number of elements 1 752. The mesh model is shown in Fig. 5.

Material properties (magnetic reluctivity) are as-

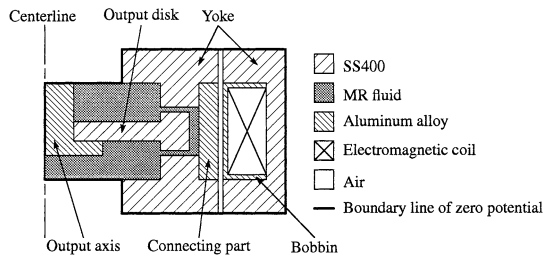


Fig. 4 Materials used in nominal MR-fluid actuator

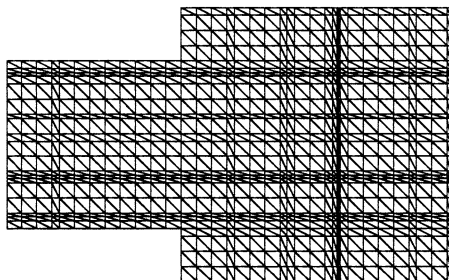


Fig. 5 Mesh model of MR-fluid actuator

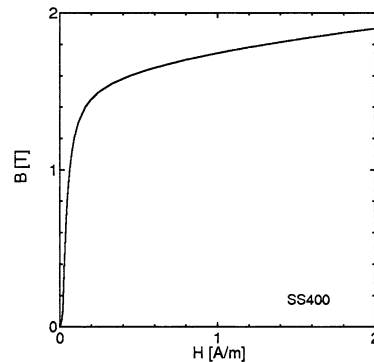
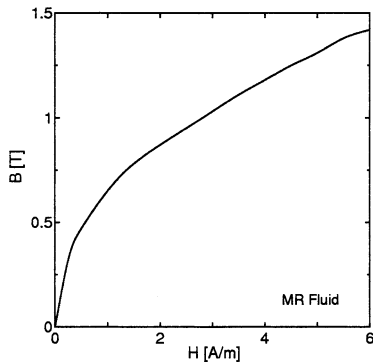


Fig. 6 $B-H$ curves of MR fluid⁽¹⁹⁾ and SS400⁽²⁰⁾

signed to each element and the calculation is carried out. Since the MR fluid and SS400, which are nonlinear materials, become the main path of flux, the $B-H$ curves^{(19), (20)} shown in Fig. 6 are used. The permeabilities of aluminum and the air gap are set to 1 as linear materials.

The result of the static magnetic analysis is shown in Fig. 7. Because the material properties used in previous work were changed, there are small differences in the figure. However, it can be confirmed that the flux passes through the MR fluid and SS400.

3.2 Dynamic analysis in consideration of eddy current

When the magnetic flux density passing through the electric conductor changes, electromotive force is induced and the eddy current passes through the conductor. Due to the eddy current, a counter-magnetic field that opposes the change in flux is produced and the response becomes slower. The time response of the magnetic field can be simulated by considering the eddy current. Therefore, the transient analysis is examined next.

3.2.1 Equation in axisymmetric three-dimensional field involving eddy current⁽²¹⁾ When the magnetic flux changes in the electric conductor (electric conductivity σ), electromotive force is induced. The electromotive force generates the eddy current. The density of eddy current J_e is given as

$$J_e = -\sigma \frac{\partial A}{\partial t} - \sigma \text{grad} \phi, \tag{1}$$

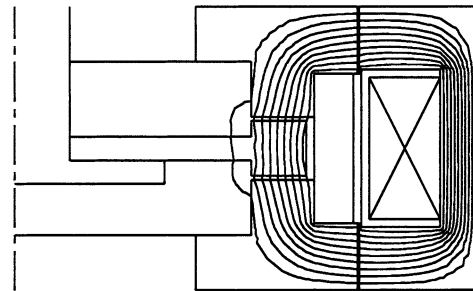


Fig. 7 Magnetic flux lines in nominal MR-fluid actuator

where A is the magnetic vector potential, and ϕ is the electric potential.

The density of current in the eddy current field \mathbf{J} is expressed as $\mathbf{J} = \mathbf{J}_0 + \mathbf{J}_e$ with the density of forced current \mathbf{J}_0 and the density of eddy current \mathbf{J}_e . Since $\text{grad}\phi$ can be set to zero in an axisymmetric three-dimensional field⁽²⁰⁾, the equation in the axisymmetric three-dimensional field involving eddy current is written as⁽²¹⁾

$$\frac{\partial}{\partial r} \left\{ \frac{v_z}{r} \frac{\partial}{\partial r} (rA_\theta) \right\} + \frac{\partial}{\partial z} \left(v_r \frac{\partial A_\theta}{\partial z} \right) = -J_{0\theta} + \sigma \frac{\partial A_\theta}{\partial t}. \quad (2)$$

The second term on the right side is related with the eddy current, but the equation of axisymmetric three-dimensional static magnetic field does not have this term. The FEM analysis program is formulated based on the above equation, and the magnetic analysis is examined.

3.2.2 Material properties In the static analysis, the reluctivity ν (the inverse of permeability μ) is necessary. On the other hand, the electric conductivity σ is additionally required for dynamic analysis. The electric conductivities of the materials used in this study are listed in Table 1. The electric conductivity is the inverse of resistivity [Ωm].

In the table, 100 IACS% (international annealed copper standard) is a value equivalent to the electric conductivity of the annealed copper standard (resistivity 17.241×10^{-9} [Ωm]). Since the electric conductivity of the materials around the coil and magnetic path influences the magnetic response, it must be used carefully.

3.2.3 Comparison between analysis and experiment The analytical and experimental results are shown in Fig. 8. Here, the vertical axis is normalized by

Table 1 Conductivities used in analysis

Material	Conductivity [$\times 10^7$ 1/ Ωm]
SS400	0.648 ⁽²⁰⁾
MR fluid	0
Aluminum alloy	1.972 (34 IACS%)
Air	0

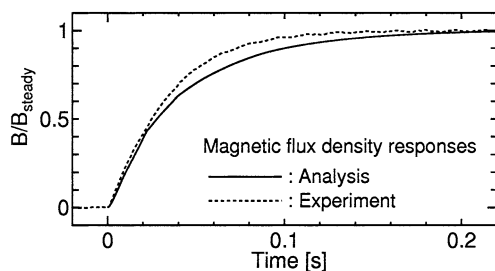


Fig. 8 Analytical and experimental magnetic flux density of nominal MR-fluid actuator

the steady-state value in order to compare the response forms.

Although the analyzed model contains modeling errors in the material properties and parts shapes, the analytical response is in good agreement with the experimental one. It can be said that the magnetic response can be estimated by the transient magnetic analysis taking into consideration the eddy current.

3.2.4 Eddy current density The eddy current caused in each part can also be determined by the above analysis. The distribution of the eddy current at 10 ms is shown in Fig. 9.

In order to concentrate the magnetic flux to the MR fluid, SS400, which is a magnetic material, was used for the yoke and a nonmagnetic aluminum alloy was used for the connecting part and the bobbin. The yoke made of SS400 was the magnetic flux path and the flux was concentrated to the MR fluid, as shown in Fig. 7. From the distribution of eddy current, however, it can be seen that a large current arises in the connecting part and the bobbin made of aluminum. This may delay the magnetic response.

4. Improvement of Response Time by Changing Material

4.1 Reduction of eddy current

Reducing the eddy current in the parts made of aluminum may be a solution for improving the response, on the basis of the distribution in Fig. 9. In order to reduce the eddy current in the aluminum part, a material that has low conductivity is required. The conductivity of the aluminum alloy used is 1.972×10^7 [1/ Ωm], about one-third of 100 IACS%, hence it may be a high conductivity material. In this case, the connecting part and bobbin need not be aluminum as long as they are nonmagnetic materials. Therefore, they were changed to nonmagnetic materials and insulators in order not to cause the eddy current. The actuator with the change of materials is called advanced actuator (1) in this paper.

4.2 Analysis of magnetic response

The dynamic magnetic analysis is performed with

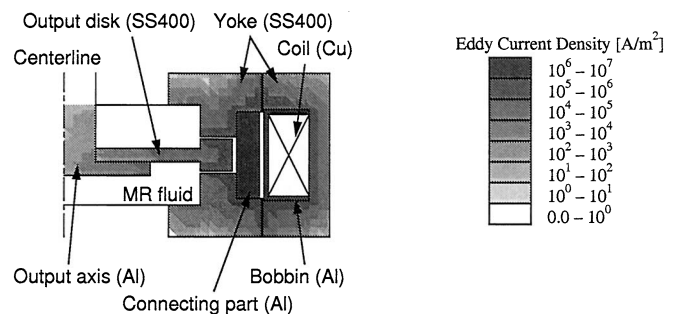


Fig. 9 Distribution of eddy-current density of nominal MR-fluid actuator

the materials of the connecting part and the bobbin being nonmagnetic materials and insulators (i.e., magnetic permeability = 1, electric conductivity = 0). The distribution of the eddy current density at 10 ms is shown in Fig. 10. As an inevitable result of the materials change to insulators, it can be seen that the eddy current is not generated in the connecting part or the bobbin. The magnetic responses before and after the change are shown in Fig. 11. From the analytical results, the magnetic response is expected to improve sharply in advanced actuator (1).

4.3 Experiment of magnetic response

Next, the magnetic flux density is measured experimentally after the connecting part and the coil bobbin are changed to cast nylon and Bakelite, respectively. The experimental results before and after the change are shown in Fig. 12. As expected from the predicted result shown in Fig. 11, the magnetic response is significantly improved. The time constant is about 7 ms.

4.4 Experiment of torque response

An experiment for assessing the torque response from the coil current is also carried out. The results before and after the change are shown in Fig. 13. The response of

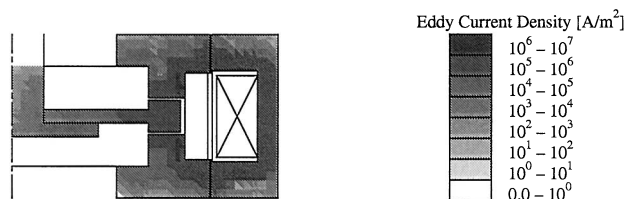


Fig. 10 Distribution of eddy-current density of advanced actuator (1)

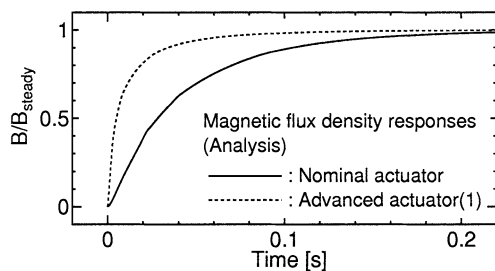


Fig. 11 Analytical magnetic flux density of advanced actuator (1)

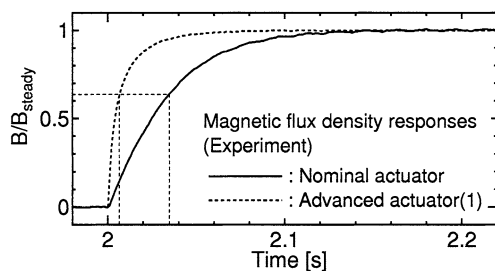


Fig. 12 Experimental magnetic flux density of advanced actuator (1)

the torque is also improved and the time constant is 12 ms, approximately one-fourth of the nominal value.

In former studies on equipment using MR fluid, aluminum or brass, as nonmagnetic material, was used for parts not included in flux path. In term of the static properties, it can be said that aluminum or brass plays the original role as nonmagnetic material. As seen from the present results, it is possible to realize a high-speed response using nonmagnetic material and an insulator, depending on the structure of the equipment.

5. Improvement of Response Time by Changing the Shape

5.1 Reduction of counter-magnetic flux

As described in the previous section, the eddy current was reduced by changing the material. As a result, counter-magnetic potential and flux were reduced, and an improvement of response time was realized. From a different point of view, it can be considered that this improvement is realized also by reducing the counter-magnetic flux itself. In this section, the shape of advanced actuator (1), in which aluminum was changed to plastic, is also changed so that the magnetic reluctance is increased in order to reduce the counterflux. The actuator with the changed shape is called advanced actuator (2).

5.2 Change of shape

In the magnetic circuit method, the magnetic reluctance is expressed as

$$R = \frac{l}{\mu S}, \quad (3)$$

where l [m] is the length of the magnetic-flux path, S [m²] is the cross-sectional area and μ [H/m] is the magnetic permeability.

It can be said that the magnetic reluctance is increased and the counterflux is reduced by decreasing the area through which it passes. Therefore, an improvement of response is expected. Then, the shape of the yoke of the input component is changed, as shown in Fig. 14. The widths of the inside regions in contact with the MR fluid are decreased by 4 mm, and the width of the upper and lower regions in contact with the air gap, by 4.5 mm.

Since these portions touch the MR fluid and air, respectively, they are the parts whose magnetic reluctance

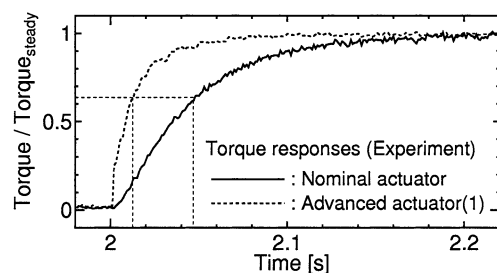


Fig. 13 Experimental torque of advanced actuator (1)

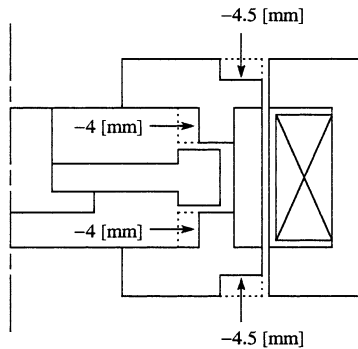


Fig. 14 Change of size of input part

tends to increase upon size changes. The total magnetic reluctance increases approximately twofold in this case. Although the magnetic flux induced by the coil current is also decreased, the magnetic flux density in the fluid seldom changes since the area of the magnetic field applied to the MR fluid also decreases. Note that the output torque may decrease because of the reduction in shearing area.

Due to the change of shape, the electric resistance may also increase because the sectional area of portions through which the eddy current passes, are reduced. Therefore, it can be considered that this shape change causes not only reduction of the counterflux via the increase of magnetic reluctance, but also the reduction of the eddy current via the increase of electric resistance.

5.3 Static magnetic analysis

The static magnetic analysis is performed after the FEM model is updated to accommodate above changes. The flux lines are shown in Fig. 15. From the figure, it is seen that the sufficient magnetic flux is applied between the input and output disks.

5.4 Transient magnetic analysis

The dynamic magnetic analysis is performed with the model including the shape change. The result is shown in Fig. 16, together with the previous results. It can be confirmed that the response is further improved in advanced actuator (2).

5.5 Experiment of magnetic response

The input disks of the actual actuator were changed. The magnetic flux density measured experimentally is shown in Fig. 17, together with the previous results. The experimental results are in good agreement with the analytical results. This confirms that the change in shape improves the response. As a result, the time constant became about 2 ms in this experiment.

5.6 Experiment of torque response

Finally, the experiment on step response from the coil current to the torque is carried out. The result and the previous results are shown in Fig. 18. As seen in the figure, improvement of the torque response was also realized, and the time constant of the torque response finally became about 5 ms, one-ninth that of the origin.

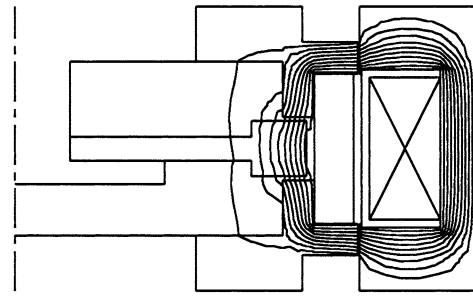


Fig. 15 Magnetic flux lines in advanced actuator (2)

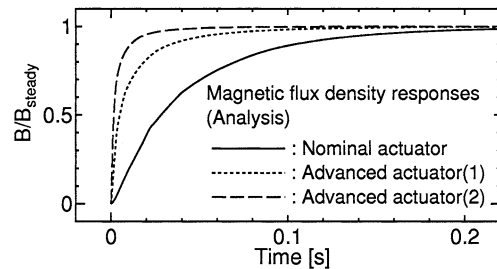


Fig. 16 Analytical magnetic flux density of advanced actuator (2)

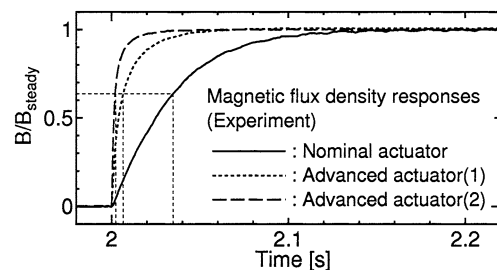


Fig. 17 Experimental magnetic flux density of advanced actuator (2)

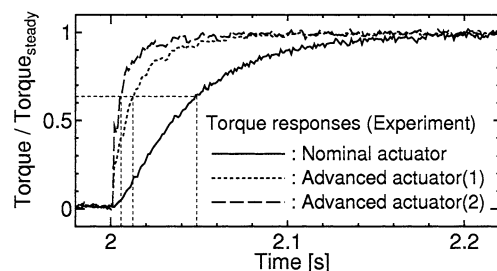


Fig. 18 Experimental torque of advanced actuator (2)

The time constants of the magnetic flux density and the output torque obtained in this study are summarized in Table 2. It is necessary to investigate the details of the relationships between the magnetic field and torque responses.

6. Basic Characteristics of Advanced MR-Fluid Actuator (2)

Finally, the basic characteristics of advanced actuator (2) are experimentally investigated. Current step response, torque-current response, torque-input speed response and

Table 2 Time constants of experimental responses

	Nominal	Advanced(1)	Advanced(2)
Current	< 1 [ms]	< 1 [ms]	< 1 [ms]
Magnetic flux density	36 [ms]	7 [ms]	2 [ms]
Torque	45 [ms]	12 [ms]	5 [ms]

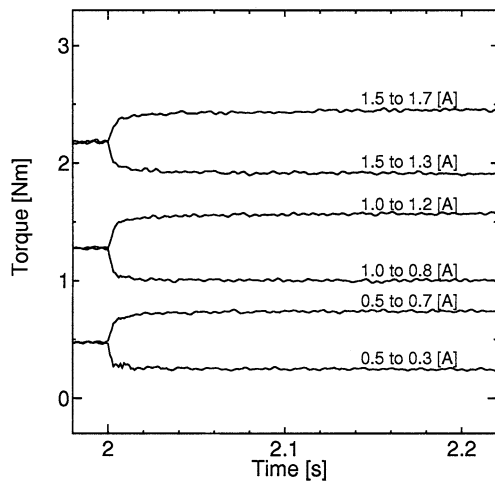


Fig. 19 Step responses of advanced actuator (2)

frequency response are examined.

6.1 Coil current step responses

The output torque is measured when a step current is input to the coil. The currents of 0.5, 1.0, and 1.5 A are changed by plus or minus 0.2 A at 2.0 s. The experimental results are shown in Fig. 19. It can be confirmed that fast responses with the same waveform were obtained.

6.2 Torque–coil current response

The torque is measured with the current changed from 0 through to 2 to 0 A twice. It takes 6.0 s to complete one cycle. The result is plotted in Fig. 20. This diagram shows a small hysteresis loop. A torque of 3 N·m is output with a current of 2 A.

6.3 Torque–input speed responses

The influences of the input speed on the output are investigated. The speed of the input part is changed from 0 through to 50 to 0 rpm twice. The torque responses are shown in Fig. 21. The coil currents were set to 0, 0.5, 1.0, 1.5, and 2.0 A. From these results, the influences on the torque were seldom observed for speeds over 10 rpm.

6.4 Frequency response from coil current to torque

Finally, the experiment on the frequency response from the coil current to the torque is performed. The input current is given as a sinusoidal wave: $0.75 +$

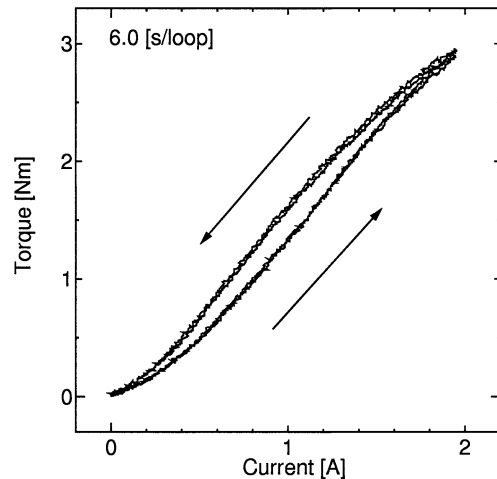


Fig. 20 Torque–current diagram of advanced actuator (2)

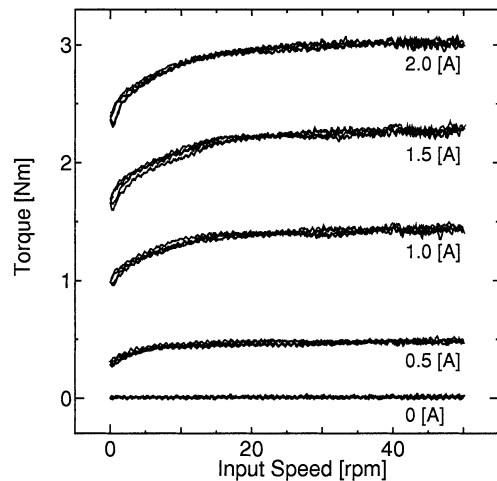


Fig. 21 Torque–speed diagram of advanced actuator (2)

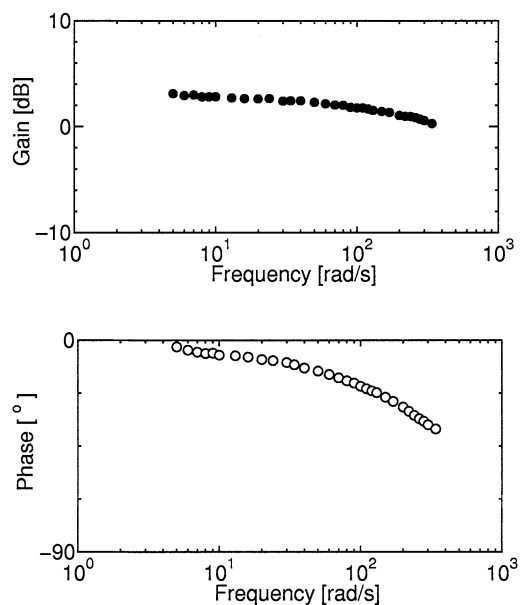


Fig. 22 Frequency response of advanced actuator (2)

$0.25 \sin(\omega t)$ [A]. The Bode diagram obtained by FFT analysis is shown in Fig. 22. It can be seen that the bandwidth extends to a high frequency of over 200 rad/s.

7. Conclusions

(1) The torque generation mechanism of the MR-fluid actuator was considered. The responses from the coil current, the magnetic flux density and the output torque were measured, and the response speeds were compared.

(2) The magnetic analyses were performed by FEM. By static analysis, it was verified that the portions made of MR fluid and SS400 formed a flux path. In the transient analysis with the eddy current taken into consideration, the magnetic responses were in good agreement with the experimental results. From the distribution of the eddy-current density, it was found that much of the eddy current passed through the parts made of aluminum alloy.

(3) In order to reduce the counter-magnetic potential due to the eddy current, aluminum in the connecting part and bobbin was changed to engineering plastic, a nonmagnetic material and an insulator. It was confirmed that the analytical and experimental magnetic responses were significantly improved, and that the torque response was also effectively accelerated by the change.

(4) In order to reduce the counterflux itself, the shape of the yoke was changed so that the magnetic reluctance was increased. It was verified that the magnetic responses were further improved, and high-speed torque responses were realized.

(5) Finally, current step response, torque-current response, torque-input speed response and frequency response were examined, and the properties of advanced actuator (2) were shown.

Acknowledgement

This study was supported by a Grant-in-Aid for Scientific Research from the Ministry of Education, Culture, Sports, Science and Technology of Japan (No.12555073).

References

- (1) Rabinow, J., The Magnetic Fluid Clutch, AIEE Transactions, Vol.67 (1948), pp.1308–1315.
- (2) Carlson, J.D., Catanzarite, D.M. and St. Clair, K.A., Commercial Magneto-Rheological Fluid Devices, Proceedings of 5th International Conference on Electro-Rheological Fluids, Magneto-Rheological Suspensions and Associated Technology, (1995), pp.20–28, World Scientific.
- (3) Jolly, M.R., Bender, J.W. and Carlson, J.D., Properties and Applications of Commercial Magnetorheological Fluids, Journal of Intelligent Material Systems and Structures, Vol.10, No.1 (1999), pp.5–13.
- (4) Carlson, J.D. and Jolly, M.R., MR Fluid, Foam and Elastomer Devices, Mechatronics, Vol.10 (2000), pp.555–569.
- (5) Ashour, O., Rogers, C.A. and Kordonsky, W., Magnetorheological Fluids: Materials, Characterization, and Devices, Journal of Intelligent Material Systems and Structures, Vol.7, No.2 (1996), pp.123–130.
- (6) Kordonsky, W.I. and Demchuk, S.A., Additional Magnetic Dispersed Phase Improves the MR-Fluid Properties, Journal of Intelligent Material Systems and Structures, Vol.7, No.5 (1996), pp.522–525.
- (7) Bölter, R. and Janocha, H., Design Rules for MR Fluid Actuators in Different Working Modes, Proceedings of SPIE the International Society for Optical Engineering, Vol.3045 (1997), pp.148–159.
- (8) Jeon, D., Park, C. and Park, K., Vibration Suppression by Controlling an MR Damper, Proceedings of the 6th International Conference on Electro-Rheological Fluids, Magneto-Rheological Suspensions and Their Applications, (1997), pp.853–860.
- (9) Choi, S.B., Hong, S.R. and Cheong, C.C., Comparison of Field-Controlled Characteristics between ER and MR Clutches, Journal of Intelligent Material Systems and Structures, Vol.10, No.8 (1999), pp.615–619.
- (10) Muriuki, M. and Clark, W.W., Design Issues in Magnetorheological Fluid Actuators, Proceedings of the SPIE Conference on Passive Damping and Isolation, Vol.3672 (1999), pp.55–64.
- (11) Yalcintas, M., Magnetorheological Fluid Based Torque Transmission Clutches, Proceedings of the International Offshore and Polar Engineering Conference, Vol.4 (1999), pp.563–569.
- (12) Yokota, S., Yoshida, K. and Kondo, Y., A Pressure Control Valve Using MR Fluid (Proposition and Basic Experiments), Proceedings of Jpn. Soc. Mech. Eng. 76th Fall Annual Meeting (IV), (in Japanese), (1998), pp.190–191.
- (13) Saito, G. and Ikeda, H., A Model for Control System Design of Actuators by Using Magneto-Rheological Suspension, Proceedings of Jpn. Soc. Mech. Eng. RoboMec '01, (in Japanese), (2001), 1A1-D9.
- (14) Yokota, M., Shiraiishi, T., Tsuchiya, T. and Morishita, S., An Application of MR-Fluid to Clutch Mechanism, Proceedings of Jpn. Soc. Mech. Eng. RoboMec '01, (in Japanese), (2001), 1A1-D10.
- (15) Asaoka, H., Lin, J., Sakaguchi, M., Zhang, G. and Furusho, J., Basic Study on Development of MR Actuator, Proceedings of Jpn. Soc. Mech. Eng. RoboMec '99, (in Japanese), (1999), 2P1-48-068.
- (16) Lin, J., Asaoka, H., Sakaguchi, M., Zhang, G. and Furusho, J., Applying Study Connected with Development of New Actuator Using MR Fluid, Proceedings of the 2000 Japan-USA Flexible Automation Conference, Vol.1 (2000), pp.413–416.
- (17) Takesue, N., Sakaguchi, M. and Furusho, J., Improvement of Response Properties of MR-Fluid Actuator by Torque Feedback Control, Proceedings of IEEE International Conference on Robotics and Automation, Vol.4 (2001), pp.3825–3830.
- (18) Takesue, N., Furusho, J., Sakaguchi, M. and Kiyota, Y., Development and Control Experiments of MR-Fluid Actuator, Trans. of Jpn. Soc. Mech. Eng., (in Japanese), C, Vol.67, No.663 (2001), pp.3525–3532.

- (19) Magneto Rheological Fluid MRF132-LD Product Bulletin, (1999), Lord Corporation.
 - (20) Takahashi, N., Jikaikei Yugen-yosoho wo Mochiita Saitekika, (in Japanese), (2001), Morikita Shuppan Co., Ltd.
 - (21) Nakata, T. and Takahashi, N., Denki-kogaku no Yugen-yosoho, (in Japanese), (1982), Morikita Shuppan Co., Ltd.
 - (22) Ohkawa, M., Eikyu-jishaku-jiki-kairo Nyumon, (in Japanese), (1994), Sogo Electronics Press.
 - (23) Chikazumi, S., Kyo-jiseitai no Butsuri (Jo), (in Japanese), (1978), Shokabo Publishing Co., Ltd.
 - (24) Konuma, M., Jisei-zairyō, (in Japanese), (1996), Kougakutosho Ltd.
 - (25) Uchiyama, S. and Masuda, M., Magnetic Materials, (in Japanese), (1980), Corona Publishing Co., Ltd.
-